BIOCHEMISTRY
including biophysical chemistry & molecular biology
Article

Biochemistry **2010,** *49,* 8085–8093 8085
DOI: 10.1021/bi100895j

Brønsted Analysis and Rate-Limiting Steps for the T5 Flap Endonuclease Catalyzed Hydrolysis of Exonucleolytic Substrates†

Blanka Sengerová,[‡,∥] Christopher Tomlinson,[‡] John M. Atack,[‡] Ryan Williams,[‡,⊥] Jon R. Sayers,[§] Nicholas H. Williams,[‡] and Jane A. Grasby*[,‡]

[‡]*Centre for Chemical Biology, Department of Chemistry, University of Sheffield, Sheffield S3 7HF, U.K., and* [§]*Henry Wellcome Laboratories for Medical Research, University of Sheffield School of Medicine and Biomedical Science, Beech Hill Road, Sheffield S10 2RX, U.K.* [∥]*Current address: Weatherall Institute of Molecular Medicine, University of Oxford, John Radcliffe Hospital, Oxford OX3 9DS, U.K.* [⊥]*Current address: Samuel Lunenfeld Research Institute, Mount Sinai Hospital, 600 University Ave., R988 Toronto, Ontario, Canada M5G 1X5.*

Received June 3, 2010; Revised Manuscript Received August 4, 2010

ABSTRACT: During replication and repair flap endonucleases (FENs) catalyze endonucleolytic and exonucleolytic (EXO) DNA hydrolyses. Altering the leaving group pK_a, by replacing the departing nucleoside with analogues, had minimal effect on k_{cat}/K_M in a T5FEN-catalyzed EXO reaction, producing a very low Brønsted coefficient, β_{lg}. Investigation of the viscosity dependence of k_{cat}/K_M revealed that reactions of EXO substrates are rate limited by diffusional encounter of enzyme and substrate, explaining the small β_{lg}. However, the maximal single turnover rate of the FEN EXO reaction also yields a near zero β_{lg}. A low β_{lg} was also observed when evaluating k_{cat}/K_M for D201I/D204S FEN-catalyzed reactions, even though these reactions were not affected by added viscogen. But an active site K83A mutant produced a $\beta_{lg} = -1.2 \pm 0.10$, closer to the value observed for solution hydrolysis of phosphate diesters. The pH−maximal rate profiles of the WT and K83A FEN reactions both reach a maximum at high pH and do not support an explanation of the data that involves catalysis of leaving group departure by Lys 83 functioning as a general acid. Instead, a rate-limiting physical step, such as substrate unpairing or helical arch ordering, that occurs after substrate association must kinetically hide an inherent large β_{lg}. It is suggested that K83 acts as an electrostatic catalyst that stabilizes the transition state for phosphate diester hydrolysis. When K83 is removed from the active site, chemistry becomes rate limiting and the leaving group sensitivity of the FEN-catalyzed reaction is revealed.

Flap endonucleases (FENs)[1] are divalent metal ion dependent DNA replication and repair nucleases that possess multiple DNA hydrolyzing activities. FENs catalyze both structure-specific endonucleolytic and 5′-exonucleolytic reactions (*1*−*3*). Endonucleolytic reactions occur on bifurcated nucleic acid structures with a region of 5′-single-stranded nucleic acid (FLAP-ENDO) or where the 5′-portion of the substrate is gapped and contains a region of duplex. Exonucleolytic (EXO) reactions are observed on double-stranded nucleic acids, such as duplex or nicked DNA. A characteristic of both FLAP-ENDO and EXO reactions is that the major site of hydrolysis occurs one nucleotide into the downstream duplex (*2*, *4*). Alongside structural promiscuity, FENs also accept substrates containing both 2′-deoxyribonucleotides and ribonucleotides (*5*). All FEN activities proceed from the same active site.

Two X-ray structures of FENs in complex with DNA exist, but neither contained bound metal ions or substrate positioned within the active site (*6*, *7*). Together with functional data, these have provided a broad understanding of how the various FEN activities arise from the same protein and active site although a detailed understanding of how FEN functions on these varying substrates remains elusive (*8*). The combined studies define the binding sites for the portions of substrates that are upstream and downstream as the N-terminal and C-terminal regions of the protein, respectively (Figure 1A).

Structural work has also revealed that all FENs contain a helical arch or clamp that forms a hole in the protein (*6*, *9*) (Figure 1A), although the role of this domain is still debated (*8*, *10*). In some structures, including the complex of T4FEN bound to pseudo-Y DNA, this arch is partially disordered (*7*). The active site is at the base of this arch. The active sites of all FENs contain seven positionally conserved carboxylates that ligand essential cofactors with an eighth carboxylate present in lower organism FENs such as that of bacteriophage T5 (*8*) (Figure 1B). A spatially conserved lysine (K83 in T5FEN), located at the base of the arch, also protrudes into the active site. Substrate-free structures of FENs from a range of sources contain two active site divalent metal ions although their spacing is variable (*8*). Functional data implicate at least three divalent metal ions in the overall reaction catalyzed by wild-type (WT) T5FEN (*11*). It is plausible that T5FEN uses a type of two metal ion mechanism for chemical rate acceleration. It is likely that metal ion 2 (Figure 1B), observed in substrate-free T5FEN structures, plays a substrate binding or structural role but does not substantively contribute to chemical catalysis.

†This work was funded by BBSRC Grants B20079 and F0147321.
*To whom correspondence should be addressed: e-mail, j.a.grasby@sheffield.ac.uk; phone, +44 114 2229478; fax, +44 114 2229346.

[1]Abbreviations: AP, alkaline phosphatase; FEN, flap endonuclease; ES, enzyme−substrate complex; [E], initial concentration of enzyme; EXO, double-stranded exonucleolytic (reaction) of a double-stranded substrate; EXO-1, exonuclease-1; FLAP-ENDO, flap endonucleolytic (reaction) of a 5′-flap substrate; GEN-1, XPG-like gap endonuclease (putative human Holliday junction resolvase); LFER, linear free energy relationship; S, substrate; [S], initial concentration of substrate; WT, wild type; XPG, xeroderma pigmentosum complementation group G.

Published on Web 08/10/2010

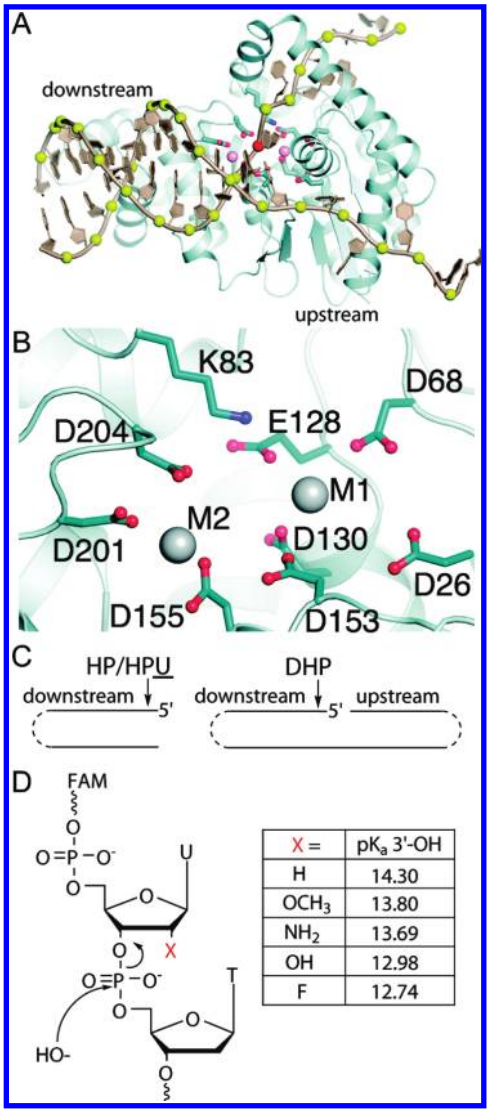

FIGURE 1: (A) A model of T5FEN bound to pseudo-Y DNA constructed from the T4RNase H pseudo-Y DNA complex (2ihn.pdb) overlaid with the crystal structure of T5FEN (1ut5.pdb) by alignment of the two proteins (T4-protein not shown). The portion of the pseudo-Y DNA substrate downstream of the major site of reaction (phosphate indicated as red sphere) is bound to the C-terminal domain of the protein, whereas the upstream 3′-single-stranded overhang is bound to the N-terminal domain. In the T4RNase H−DNA complex a portion of the helical arch is disordered. In the superposition with T5FEN, which was crystallized with an ordered helical arch, the 5′-single-stranded portion of the pseudo-Y substrate appears to pass through the helical arch. (B) Close-up of the T5FEN (1ut5.pdb) active site showing T5FEN-bound metal ions M1 and M2 are represented as gray spheres. Crystallized bacteriophage FENs (T5 and T4) possess eight active site carboxylates, seven of which are structurally conserved in FENs from all sources (D26, D68, E128, D130, D153, D155, D204), although at some positions interchanges of Glu and Asp residues are observed. K83 is positionally conserved in all FENs (Figure S4 in Supporting Information). (C) The structures of the EXO hairpin substrates HP and HPU and the nicked DNA double hairpin substrate DHP used in this study. Hairpin turns are included to minimize the number of EXO reaction sites. An arrow indicates the major site of reaction one nucleotide into the double-stranded region. The sequences used to construct these oligomers are given in Table 1. (D) To study the relationship between rate of the FEN-catalyzed reaction and pK_a of the leaving group, hairpin EXO substrates (HPU where U is the site of modification) were created where the terminal nucleoside was 2′-deoxyuridine, 2′-deoxy-2′-*O*-methyluridine, 2′-deoxy-2′-aminouridine, uridine, or 2′-deoxy-2′-fluorouridine. The pK_as of the 3′-OH group used are those of the respective modified adenosine triphosphates (*23*).

Studies on the effects of changing the leaving group pK_a on the reaction rate, known as Brønsted plots or more generally linear free energy relationships (LFER), can be used to quantify the charge changes that occur at the leaving group on going from the ground state to the transition state (*12*), allowing an insight into the nature of the enzyme-catalyzed reaction. Exploiting the lack of nucleotide specificity exhibited by FENs, we varied the pK_a of the leaving group in the EXO reactions of WT and mutated FENs by changing the 2′-substituent of the ribose moiety. With the exception of a K83A mutant FEN, these changes had surprisingly little impact on the reaction rate constants. This prompted us to question whether physical steps such as enzyme substrate association could be rate limiting under subsaturating conditions of enzyme and substrate. However, even when reactions were examined under conditions where diffusional encounter of enzyme and substrate was not rate limiting, insensitivity to leaving group pK_a was still observed. The implications of these results for catalysis by FEN are examined.

MATERIALS AND METHODS

Enzyme and Substrates. The D201I/D204S T5FEN mutant was constructed as described for a N-terminal truncated variant (*13*) but in the context of the full-length protein. K83A T5FEN has been reported earlier (*14*−*16*). Wild-type (WT) T5FEN and mutants were overexpressed and purified to homogeneity essentially as described previously (*17*) followed by an additional chromatography step employing Q-Sepharose using buffer A (25 mM Tris-HCl (pH 8.0), 1 mM DTT, 1 mM EDTA, and 5% glycerol containing 50 mM NaCl). Fractions were eluted using a linear salt gradient (50−1000 mM), and those found to contain pure T5FEN, based on SDS−PAGE, were buffer exchanged into buffer A using a VivaSpin device (Vivascience) and diluted 1:1 in glycerol for storage at −20 °C. The concentration of protein was determined using the Bradford assay.

The substrates (Table 1) were synthesized and purified as described (*2*). Modified substrates (HPU, FAM-Ud(TACACACGCTTGCGTGTGTAA), Figure 1C,D, where U is 2′-deoxyuridine, 2′-deoxy-2′-*O*-methyluridine, 2′-deoxy-2′-aminouridine, uridine, and 2′-deoxy-2′-fluorouridine) were synthesized using reagents supplied by Glen research (via Cambio), with appropriate modification to synthesis and deprotection procedures according to the manufacturer's instructions, and were purified analogously. All oligonucleotides were characterized by MALDI-TOF mass spectrometry and molecular weights were in good agreement with their calculated values.

Determination of k_{cat}/K_M. Reaction mixtures containing appropriate concentrations of FAM-labeled substrates in 25 mM potassium glycinate or CHES (pH 9.3) or 25 mM MES (pH 6.5) and 50 mM KCl were heated to 95 °C for 1 min and cooled to 37 °C to prefold the substrate. Reactions (25 mM potassium glycinate or CHES (pH 9.3) or 25 mM MES (pH 6.5), 50 mM KCl, 0.01 mg/mL BSA, 10 mM $MgCl_2$) were initiated by addition of enzyme, sampled at eight appropriate time intervals (125 μL aliquots) and quenched with excess EDTA (200 mM, 25 μL) and the amount of substrate and products determined using dHPLC (Wave fragment analysis system with a fluorescence detector; Transgenomic) as described (*2*). The final concentrations of substrates ranged 5−50 nM HP (pH 9.3), 0.5−5 nM HP (pH 6.5), 5−20 nM DHP, and 1−20 nM HPU so that in all cases [S] < K_M, and the final concentration of enzyme was varied (2−500 pM) dependent on the rate of reaction.

Table 1: Sequences of FEN Substrates[a] Used in This Study

substrate	sequence
HP	FAM-d(GAACACACGCTTGCGTGTGTTC)
HPU	FAM-Ud(TACACACGCTTGCGTGTGTAA)
DHP	FAM-d(GAACACACGCTTGCGTGTGTTCCACAACATAGAGATATGTTGTG)

[a]See Figure 1C,D.

Normalized initial rates of reaction (v/[E]) at varying substrate concentrations were determined, and the slope of a plot of v/[E] versus [S] was used to determine k_{cat}/K_M.

The effects of added viscogen (sucrose, 0−35%, w/v) on k_{cat}/K_M were determined using sucrose-containing buffers and the same procedure. The relative solvent viscosity (η/η^0) of each buffer solution containing sucrose was determined using an Ostwald viscometer immersed in a water bath at 37.0 °C as described (*18*). The relative viscosities measured were 1.02, 1.34, 1.45, 1.70, 2.00, 2.44, 2.95, 3.32, 3.38, and 3.89 for 0%, 10%, 13%, 18%, 20%, 25%, 30%, 31%, 33%, and 35% (w/v) sucrose solutions, respectively.

Determination of k_{STmax}. Rapid-quench experiments were carried out at 37 °C using a RQF-63 device from Hi-Tech Ltd. (Salisbury, U.K.) as described (*19*, *20*). Enzyme (supplied at saturation, 1−3 μM dependent on pH) in reaction buffer (25 mM potassium glycinate (pH 9.3) or 25 mM MES (pH 6.5 and 5.5), 10 mM $MgCl_2$, 50 mM KCl, 0.01 mg/mL BSA) was mixed with an equal volume of prefolded substrate (2 nM) in the same buffer. Reactions were quenched (1.5 M sodium hydroxide, 20 mM EDTA) at time intervals ranging from 9.1 ms to 51.2 s. At pH 5.5 mixing and sampling were carried out manually at time intervals ranging from 8 to 960 s. Reactions were analyzed as described (*2*). In the case of $HPU_{2'OH}$ (i.e., U = rU), which contained a single ribonucleotide, the quench caused some degradation of the intact substrate, but the product FAM-p-rU was unaffected. The FAM-labeled product of hydroxide-catalyzed transesterification/hydrolysis of HP(rU) that contains an additional phosphate ester was retained more strongly than the enzymatic product on dHPLC. Thus for reactions of $HPU_{2'OH}$ the total substrate remaining in the FEN reaction was calculated from the intensity of the degradation peak plus that of the intact substrate.

pH Dependence of the Maximal Rate of the WT and K83A FEN Reactions. These experiments were conducted with saturating HP substrate (1 μM WT enzyme, 1.6 μM K83A) under multiple turnover conditions as described above using MES (pH 5.5−6.5), HEPES (pH 7.0−9.0), CHES, or potassium glycinate (pH 9.3−10.5). In the case of K83A data could only be collected to pH 6.5, due to the slowed rate of reaction. The following equations were used to fit the pH dependence of the catalytic parameters (*21*, *22*). All curve fitting was carried out using Kaleidagraph Software (Synergy Software, Reading, PA) using logged data.

Enzyme active in monoanionic form:

$$\log k_{cat} = \log \frac{k_{cat(max)} 10^{-pK_{ES}}}{10^{-pK_{ES1}} + 10^{-pH}} \quad (1)$$

Enzyme active in dianionic form:

$$\log k_{cat} = \log \frac{k_{cat(max)} 10^{-pK_{ES1}} 10^{-pK_{ES2}}}{10^{-pK_{ES1}} 10^{-pK_{ES2}} + 10^{-2pH} + 10^{-pK_{ES1}} 10^{-pH}} \quad (2)$$

where $k_{cat(max)}$ is the maximal turnover number of the enzyme and K_{ES}, K_{ES1}, and K_{ES2} are the acid dissociation constants of the ES complex.

RESULTS

Effect of Altering the pK_a of the Leaving Group on k_{cat}/K_M for the WT T5FEN-Catalyzed EXO Reaction. FEN-catalyzed phosphate diester hydrolysis produces products terminating in a 3′-hydroxyl group and 5′-phosphate (*16*). To measure the effect of varying the pK_a of the leaving group on the rate of the FEN-catalyzed reaction, substrates were created where the departing nucleoside was replaced with a modified analogue (Figure 1C,D, Table 1). Although the major reaction site in all types of substrates for T5FEN occurs one nucleotide into the downstream duplex, larger substrates can be cleaved at several additional reaction sites. This arises due to the increased potential for alternative binding modes of larger substrates to the protein and from EXO reactions at all double-stranded 5′-termini. Construction from a single oligomer using a hairpin turn can be used to create EXO substrates with only a single 5′-terminus (Figure 1C). A 5′-fluorescein- (FAM-) labeled 22-mer hairpin substrate (HP, Table 1), that occupies the downstream binding site of T5FEN, has been shown to undergo exonucleolytic hydrolysis producing mainly (>90%) single nucleotide products (FAM-p-G) with small traces of dimer products (FAM-p-G-p-A) (*2*). Therefore, the EXO substrate chosen for these studies was the 22-mer hairpin duplex (HPU, Table 1 and Figure 1D), with appropriate sequence changes to accommodate the modifications.

The pK_a of the departing 3′-hydroxyl group was varied by changing the 2′-substituent of the sugar (*23*) (Figure 1D). Fluorescent substrates were created where the 5′-terminal nucleoside was 2′-deoxyribose, 2′-deoxy-2′-*O*-methylribose, 2′-deoxy-2′-aminoribose, 2′-ribose, or 2′-deoxy-2′-fluororibose. The major product of reaction of the HPU substrates (FAM-p-U) was verified by mass spectrometry, demonstrating that reaction occurs at the site of modification and that the modifications do not alter FEN specificity (Figure S1 in Supporting Information).

The apparent second-order rate constants (k_{cat}/K_M) of FEN-catalyzed hydrolysis of the HPU substrates were determined at pH 9.3 and 6.5. These rate constants were obtained from the slope of a plot of reaction rate (normalized for enzyme concentration) versus substrate concentration ([S]) under conditions where [E] ≪ [S] < K_M. Full steady-state analyses (Figure S2 in Supporting Information) indicate that the HPU modifications generally have relatively small effects on catalytic parameters. The slopes of the lines correlating log k_{cat}/K_M with the pK_a of the leaving group (the LFER Brønsted coefficient, β_{lg}) are very close to zero (β_{lg} = −0.09 ± 0.23 at pH 9.3 and β_{lg} = −0.11 ± 0.07 at pH 6.5), showing that the overall FEN-catalyzed reaction is almost completely insensitive to the leaving group pK_a (Figure 2A).

Is WT T5FEN-Catalyzed EXO Hydrolysis Limited by Substrate Association at Low E and S? The simplest explanation for the lack of a significant effect of the leaving group pK_a on k_{cat}/K_M is that the WT FEN-catalyzed EXO reaction is rate limited by a physical step in the catalytic cycle. The most likely candidate for this under conditions of low E and S is the association of enzyme and substrate, in which case k_{cat}/K_M measures the rate of

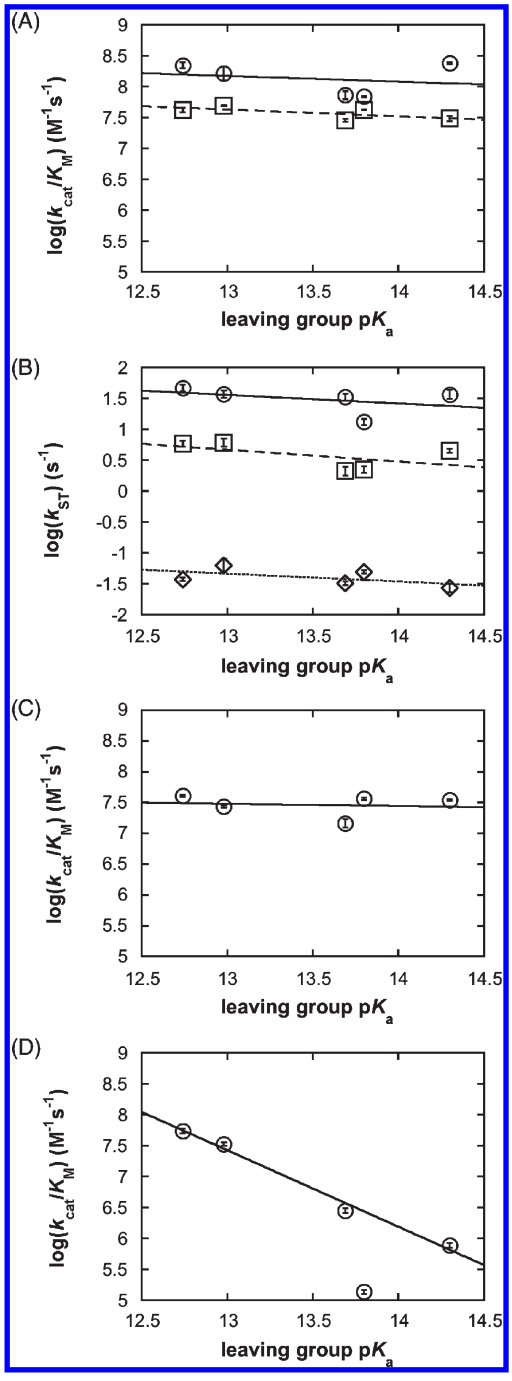

FIGURE 2: Brønsted analysis of the effect of varying the pK_a of the leaving group on the rate constant of EXO FEN reactions. The analogues used to construct the HPU substrates with the respective pK_as of their 3′-OH groups are shown in Figure 1. The slope of the straight line is β_{lg}. (A) The variation of log k_{cat}/K_M as a function of leaving group pK_a for the WT T5FEN reaction at pH 9.3 (circles), $\beta_{lg} = -0.09 \pm 0.23$, and pH 6.5 (squares), $\beta_{lg} = -0.11 \pm 0.07$. (B) The variation of log k_{ST} as a function of leaving group pK_a for the WT T5FEN reaction at pH 9.3 (circles), $\beta_{lg} = -0.14 \pm 0.17$, pH 6.5 (squares), $\beta_{lg} = -0.19 \pm 0.17$, and pH 5.5 (diamonds), $\beta_{lg} = -0.13 \pm 0.11$. (C) The variation of log k_{cat}/K_M as a function of leaving group pK_a for the D210I/D204S mutant T5FEN reaction at pH 9.3, $\beta_{lg} = -0.04 \pm 0.16$. (D) The variation of log k_{cat}/K_M as a function of leaving group pK_a for the K83A mutant T5FEN reaction at pH 9.3, $\beta_{lg} = -1.2 \pm 0.10$. The anomalously low data point generated by $HPU_{2'OMe}$ was excluded from the fit, although its inclusion would serve to raise the magnitude of β_{lg} further. All experiments were carried out in triplicate, and standard errors are shown.

diffusional encounter of these molecules rather than the bond-breaking step. To measure the extent to which the FEN-catalyzed

Scheme 1

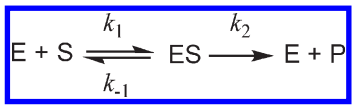

EXO reaction is diffusion controlled, the influence of added viscogen (sucrose) on the kinetic parameters was investigated. The substrates used were the unmodified EXO substrate HP that occupies only the downstream binding site of T5FEN and a longer double hairpin substrate (DHP) that occupies both upstream and downstream binding sites (mimicking a typical biological EXO substrate for FEN).

The apparent second-order rate constant (k_{cat}/K_M) for hydrolysis of HP and DHP catalyzed by T5FEN at pH 9.3 with a number of viscogen concentrations was determined using substrate concentrations below K_M. Similar experiments were also carried out at pH 6.5 for the T5FEN-catalyzed hydrolysis of HP. For a simple enzyme-catalyzed reaction that follows the pathway shown in Scheme 1, assuming that the rate of association of enzyme and substrate (k_1) and the rate of decomposition of the enzyme−substrate (ES) complex (k_{-1}) are inversely proportional to viscosity, it can be shown that

$$\frac{1}{k_{cat}/K_M} = \frac{1}{k^0{}_1}\frac{\eta}{\eta^0} + \frac{k^0{}_{-1}}{k^0{}_1 k_2} \quad (3)$$

where k_2 is the rate of conversion of ES to enzyme and products, η/η^0 is the relative viscosity of the reaction medium, and $k^0{}_1$ and $k^0{}_{-1}$ are the respective rates of association of enzyme and substrate and dissociation of the ES complex with no added viscogen (*24*). The same relationship holds for more complex kinetic schemes with additional steps after substrate association, except that the intercept becomes a more complex parameter (Figure S3 in Supporting Information).

The results of these experiments for the EXO reactions catalyzed by WT FEN are shown in Figure 3A−C, showing that in all cases the rate of reaction is affected by added sucrose. Comparable data are also obtained when glycerol is supplied as the viscogen (data not shown). Solving eq 3 for $\eta/\eta^0 = 1$ gives the apparent second-order rate constant at zero viscogen ($(k_{cat}/K_M)^0$), yielding values of $(5.4 \pm 1.9) \times 10^7$ M^{-1} s^{-1} for HP at pH 9.3, $(3.2 \pm 1.4) \times 10^7$ M^{-1} s^{-1} for HP at pH 6.5, and $(3.2 \pm 0.9) \times 10^7$ M^{-1} s^{-1} for DHP at pH 9.3. These are all in line with expected rates of diffusional encounter of biomolecules of 10^7−10^9 M^{-1} s^{-1} (*24*) and the measured rates of the FEN-catalyzed EXO reaction with no added viscogen.

To compare all of these data, a normalized plot of $(k_{cat}/K_M)^0/(k_{cat}/K_M)$ against relative viscosity is shown in Figure 4 (*25*). The expected relationship between the parameters is defined by eq 4:

$$\frac{(k_{cat}/K_M)^0}{k_{cat}/K_M} = \frac{k_2}{(k^0{}_{-1} + k_2)}\frac{\eta}{\eta^0} + \frac{k^0{}_{-1}}{k^0{}_{-1} + k_2} \quad (4)$$

For a completely diffusion-controlled reaction, $k_2 \gg k^0{}_{-1}$, and a plot of $(k_{cat}/K_M)^0{}_{calc}/(k_{cat}/K_M)$ versus η/η^0 has a slope of 1 with a near zero intercept. However, for a reaction that is not under diffusional control, $k^0{}_{-1} \gg k_2$, and the same plot will have a slope of 0 with an intercept of 1. The slopes of the normalized plots for HP and DHP at pH 9.3 are 1.10 ± 0.07 and 0.81 ± 0.05, respectively (Figure 4), and indicate that the hydrolysis of the two substrates is diffusion controlled at this pH value. At pH 6.5,

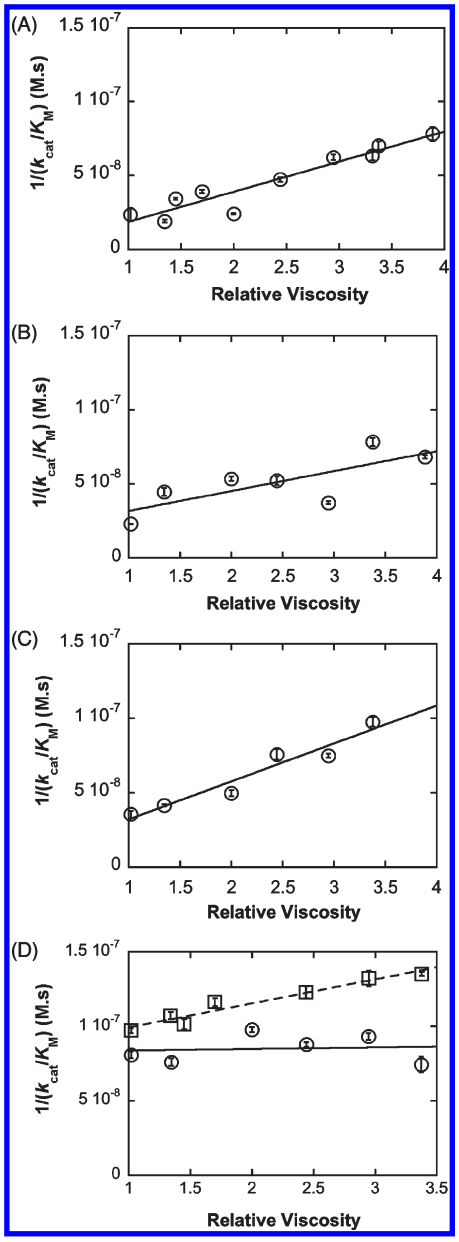

FIGURE 3: The effect of added viscogen (sucrose) on the T5FEN-catalyzed reaction of EXO substrates (A) HP at pH 9.3, (B) HP at pH 6.5, and (C) DHP at pH 9.3 and on the T5FEN mutant D210I/D204S catalyzed reaction of EXO substrates (D) HP (circles) and HP(U_{2F}) (squares) at pH 9.3, as described in Materials and Methods. Plots of $1/(k_{cat}/K_M)$ versus relative viscosity (η/η^0) according to eq 3 yield slopes of (A) $(2.04 \pm 0.24) \times 10^{-8}$ M s, (B) $(1.34 \pm 0.51) \times 10^{-8}$ M s, and (C) $(2.54 \pm 0.34) \times 10^{-8}$ M s and (D) HP $(0.10 \pm 0.51) \times 10^{-8}$ M s and $HPU_{2'F}$ $(1.62 \pm 0.18) \times 10^{-8}$ M s with intercepts of (A) $(-0.17 \pm 0.6) \times 10^{-8}$ M s and (B) $(1.84 \pm 1.33) \times 10^{-8}$ M s, and (C) $(0.66 \pm 0.79) \times 10^{-8}$ M s and (D) HP $(8.26 \pm 1.25) \times 10^{-8}$ M s and $HPU_{2'F}$ $(8.30 \pm 0.40) \times 10^{-8}$ M s. All experiments were carried out in triplicate as described in Materials and Methods, and standard errors are shown.

the normalized plot for HP hydrolysis has a slope of 0.43 ± 0.08 (Figure 4A), implying partial diffusion control.

Effect of Altering the pK_a of the Leaving Group on Maximal Single Turnover Rate (k_{STmax}) for the WT T5FEN-Catalyzed EXO Reaction. To avoid measuring the rate of diffusional encounter of E and S, the maximal rates of reaction of the enzyme−substrate complex were investigated. The maximal rate of FEN-catalyzed single turnover reactions (k_{STmax}) of HPU substrates are approximately 2-fold faster than k_{cat}, implying that

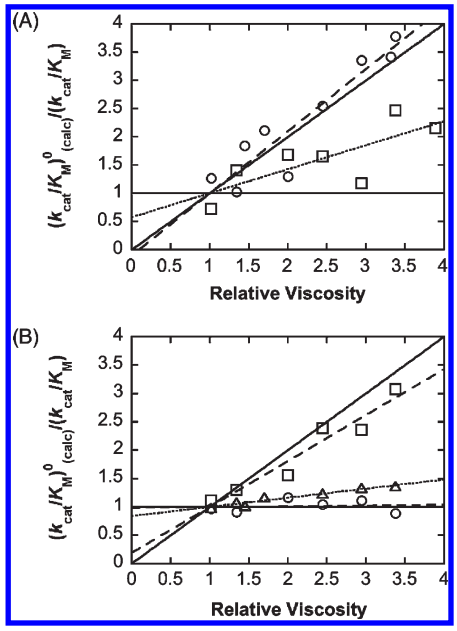

FIGURE 4: Plots of $(k_{cat}/K_M)^0_{calc}/(k_{cat}/K_M)$ versus relative viscosity (η/η^0) of reaction medium for the reaction of WT and D201I/D204S T5FENs with the specified substrates according to eq 4. Continuous lines with slopes of 1 and 0 are drawn for a completely diffusion-controlled reaction and a reaction that is not under diffusion control, respectively. (A) The slopes shown for the substrates HP, pH 9.3 (circles) = 1.1 ± 0.07, and HP, pH 6.5 (squares) = 0.43 ± 0.08, with WT T5FEN. (B) The slopes shown for the substrates DHP (squares) with WT T5FEN, pH 9.3 = 0.8 ± 0.05, HP, pH 9.3 with D201I/D204S (circles) = 0.01 ± 0.03, and $HPU_{2'F}$, pH 9.3 with D201I/D204S (triangles) = 0.16 ± 0.1.

product release partially limits the rate of reaction (Figure S2 in Supporting Information). This could suppress the observed value of β_{lg}, and so values of k_{STmax} were used to compare rates of reactions with the various modified HPU substrates. These were evaluated at three pH values: pH 9.3, where k_{STmax} is independent of pH, and pH 6.5 and 5.5, where k_{STmax} is pH dependent. Again, the measured Brønsted coefficients are all very close to zero. At pH 9.3 $\beta_{lg} = -0.14 \pm 0.17$, at pH 6.5 $\beta_{lg} = -0.19 \pm 0.17$, and at pH 5.5, $\beta_{lg} = -0.13 \pm 0.11$ (Figure 2B). Thus, even the maximal rate of the FEN-catalyzed reaction of EXO substrates is virtually insensitive to the pK_a of the leaving group.

Brønsted Coefficients and Viscogen Dependence of EXO Reactions Catalyzed by Mutated FENs. As diffusion-controlled reactions require the rates of the processes succeeding substrate association to be faster than substrate dissociation, mutants of T5FEN that are known to decrease the maximal rate of reaction were studied. A D201I/D204S double mutant brings about a 14-fold reduction in k_{STmax} with HP as substrate at pH 9.3. These mutations were chosen based on the sequence of exonuclease IX, a protein encoded by *Escherichia coli* which shares a high degree of homology with bacterial FENs but lacks the helix-three-turn-helix carboxylate residues (*26*, *27*). The loss of these carboxylates from the active site disrupts the binding of metal ion 2 observed in X-ray structures of WT FEN (Figure 1B). However, evaluation of k_{cat}/K_M for the D201I/D204S catalyzed reaction of the HPU series of substrates still produced a very low value of $\beta_{lg} = 0.05 \pm 0.22$ (Figure 2C) at pH 9.3.

The viscogen dependence of $1/(k_{cat}/K_M)$ for the D201I/D204S catalyzed reaction of HP at pH 9.3 is shown in Figure 3D and demonstrates that the rate of reaction is not altered by changes in relative viscosity. Transferring these data to a normalized plot

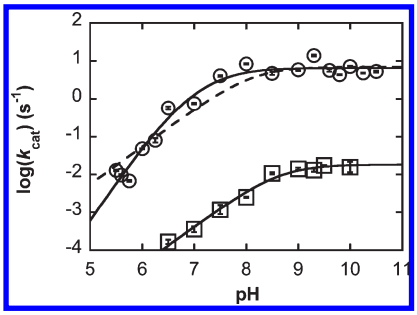

FIGURE 5: The pH dependence of k_{cat} for the WT (circles) and K83A (squares) FEN reactions. Reactions were carried out in the appropriate buffer at saturating concentrations of HP substrate as described in Materials and Methods. Data have been fitted according to eq 1 (enzyme active in monoanionic form) to yield $pK_{ES} = 8.1 \pm 0.2$ and $k_{cat(max)} = 7.1 \pm 1.9\ s^{-1}$ ($R = 0.96$) for the WT enzyme (circles, dashed line) and $pK_{ES} = 8.6 \pm 0.1$ and $k_{cat(max)} = 0.02 \pm 0.002\ s^{-1}$ ($R = 0.99$) (squares, solid line) or eq 2 (enzyme active in dianionic form) to yield $pK_{ES1} = 6.5 \pm 0.4$ and $pK_{ES2} = 7.5 \pm 0.3$ and $k_{cat(max)} = 6.5 \pm 1.2\ s^{-1}$ ($R = 0.98$) for the WT enzyme (circles, solid line).

(using $(k_{cat}/K_M)^0 = (1.2 \pm 0.2) \times 10^7\ M^{-1}s^{-1}$) produces a slope of 0.01 ± 0.03 (Figure 4B), showing that the D201I/D204S catalyzed reaction of HP is not diffusion controlled at pH 9.3. The FEN substrate that has the lowest leaving group pK_a in the HPU series, $HPdU_{2'F}$ (Figure 1D, X = F), does show a modest retardation of reaction with increasing viscosity as seen in the slope of the $1/(k_{cat}/K_M)$ plot (Figure 3D (squares)). Applying these data to a normalized plot (eq 4 $(k_{cat}/K_M)^0_{calc} = (1.0 \pm 0.1) \times 10^7\ M^{-1}s^{-1}$) gave a slope of 0.16 ± 0.02, suggesting only partial dependence of rate on substrate association and implying that in addition to substrate association other factors must also influence the rate of reaction of $HPdU_{2'F}$. Thus the near zero β_{lg} observed for the D201I/D204S catalyzed reactions cannot be explained in terms of a wholly rate-limiting diffusion-controlled process.

An alternative mutation of T5FEN, where the active site lysine 83 is altered to alanine (K83A), has a much larger impact and leads to a 1000-fold reduction in the maximal rate of reaction. In contrast to the WT and D201I/D204S T5FENs, the k_{cat}/K_M values determined for the K83A catalyzed reactions of the HPU series of substrates varied by 2 orders of magnitude. The corresponding Brønsted plot shows that the reaction is highly sensitive to the pK_a of the leaving group (Figure 2D) with $\beta_{lg} = -1.2 \pm 0.08$. However, an apparently anomalously low second-order rate constant was observed when the substrate contained the relatively bulky 2′-*O*-methyl group ($HP_{2'OMe}$), and this data point was excluded from curve fits to determine β_{lg}. If this datum is included, the apparent sensitivity would be even greater.

pH Dependence of k_{cat} for the WT and K83A T5FEN Reactions. A possible explanation for the observation that a substantial β_{lg} is only observed for the K83A catalyzed reaction is that lysine 83 acts as a general acid when it is present, protonating the leaving group as it departs and preventing any substantial charge building up at this position. To explore the ionic form of WT and K83A T5FEN required for activity, we monitored k_{cat} as a function of pH using HP as the substrate (Figure 5). Like many other metallonuclease reactions, including the FLAP−ENDO reaction catalyzed by WT T5FEN, the rate of the EXO reaction catalyzed by both WT and K83A mutant increases with pH until a pH-independent plateau is reached at higher pH. In both cases data can be fit to a single ionization model (eq 1) to yield a $pK_{ES} = 8.1 \pm 0.2$ for the WT protein and $pK_{ES} = 8.7 \pm 0.1$ for K83A. However, for the WT protein, at lower pH the reaction appears to have a second-order dependence on hydroxide ion concentration (slope of 2 in the log−log plot), and an improved fit to the data is obtained if activity is assumed to depend on the concentration of a doubly deprotonated form of the enzyme (eq 2) with $pK_{ES1} = 6.5 \pm 0.4$ and $pK_{ES2} = 7.5 \pm 0.3$, respectively. Maximal single turnover rate constants for the EXO reaction catalyzed by WT T5FEN, which are not influenced by product release steps, also display the same pH-dependent behavior (data not shown). Analogous kinetic models for catalytically competent doubly deprotonated forms of other divalent metal ion dependent nucleases have been reported, although the assignment of these pK_as to individual enzyme moieties is still debated (*28*−*30*). In the case of the very slow K83A mutant it was not possible to collect data below pH 6.5, and it is therefore impossible to distinguish between singly and doubly deprotonated catalytically competent forms.

Importantly, the pH−rate profiles observed for WT and K83A mutated FENs do not support a role for lysine 83 as a general acid in the FEN reaction. If protonation of lysine 83 were a requirement for catalysis and the protonation state of this residue was altered in the pH range tested, a decrease in activity at high pH would be expected in the profile of the WT enzyme but be absent in that of K83A. However, up to pH 10.5 there is no evidence of a downward limb in the WT pH−rate profile. The observation of pH-independent behavior in pH profiles of both WT and K83A T5FEN also rules out any possibilities of kinetic equivalence where reaction depends on a protonated state (e.g., protonated lysine) that reacts with hydroxide.

DISCUSSION

The data presented here show that the rate of WT FEN-catalyzed hydrolysis of an exonucleolytically processed substrate has little or no dependence on the pK_a of the leaving group. This is the case regardless of the pH the reaction is monitored at and whether the apparent second-order rate constant (k_{cat}/K_M) or the maximal single turnover rate constant (k_{STmax}) is measured. These data are in striking contrast to the hydrolysis of phosphate diesters in solution, which is typically very sensitive to the pK_a of the leaving group. For example, the hydroxide ion catalyzed hydrolysis of methyl aryl phosphate diesters in solution has $\beta_{lg} = -0.94 \pm 0.05$ (*31*), the hydroxide-catalyzed cleavage of uridine 3′-alkoxy phosphate diesters has $\beta_{lg} = -1.28 \pm 0.05$ (*32*), and the pH-independent hydrolysis of diaryl phosphate diesters has $\beta_{lg} = -0.97 \pm 0.05$ (*33*).

In the case of the overall WT FEN-catalyzed reaction the lack of substantive effects on the apparent second-order rate constant (k_{cat}/K_M) upon varying the leaving group is explained by a physical rate-limiting step. The effect of varying the relative viscosity of the reaction medium demonstrates that the reaction is diffusion controlled at pH 9.3. This is the case for both the shorter EXO substrate (HP) used to study the effect of leaving group departure and the longer nicked DNA substrate (DHP) that also occupies the upstream nucleic acid binding site. At pH 6.5, the maximal single turnover rate of reaction is reduced, implying that the overall rate of the processes on the reaction pathway that occur after substrate association is slowed. At this pH the FEN-catalyzed EXO reaction is partially diffusion controlled when enzyme and substrate are at low concentration, indicating that substrate dissociation and the forward reaction of the enzyme−substrate complex have similar rates (i.e., $k_{-1} \sim k_2$, Scheme 1). This means that any substantial increase in the rate of the forward

reaction of the enzyme−substrate complex through increasing the reactivity of the substrate (i.e., by lowering the leaving group pK_a) will not be fully expressed in the overall reaction parameters. That is because the substrate association step, which is insensitive to the variation in the leaving group, sets an upper limit on the apparent second-order rate constant (k_{cat}/K_M), and the reaction rate just tends to the diffusion-controlled limit as the rate of the chemical step is increased. Accordingly, the magnitude of the overall β_{lg} defined by HPU substrates with better leaving groups than 2′-deoxy alcohols is also limited to small values by the physical rate-limiting step when k_{cat}/K_M is measured at pH 6.5. Thus, all k_{cat}/K_M data for the WT protein data can explained in terms of a rate-limiting binding step that masks any impact of changing the leaving group pK_a may have on the reactivity of the enzyme−substrate complex.

In contrast, viscosity studies show that the EXO reaction catalyzed by D201I/D204S mutant FEN is not diffusion controlled. Yet evaluation of k_{cat}/K_M for the reactions catalyzed by the D201I/D204S also reveals a near zero β_{lg} that cannot be explained by the diffusion-controlled binding of substrate and enzyme. Additionally, the maximal rate of the single turnover WT FEN-catalyzed EXO reaction ($k_{ST(max)}$), evaluated with saturating enzyme concentrations, is also surprisingly insensitive to the pK_a of the leaving group and has a near zero β_{lg}. These single turnover rate constants only depend on the rate-limiting step of the enzyme−substrate complex, and so this insensitivity cannot be explained by the diffusion-controlled binding of substrate and enzyme nor the product release step. This behavior could arise because the bond cleavage step is insensitive to the nature of the leaving group or because the rate-limiting step of the enzyme−substrate complex involves a further physical process, such as a conformational change, that precedes breaking the scissile bond.

In contrast to these observations, the apparent second-order rate constant for the reaction catalyzed by the K83A mutant has a large negative $\beta_{lg} = -1.2 \pm 0.1$. Thus in the absence of lysine 83, the FEN-catalyzed reaction shows a high sensitivity to the nature of the leaving group, implying that cleavage of the scissile phosphate diester is rate limiting for the overall reaction of this mutant. This sensitivity is similar to the reactions of simple phosphate diesters in solution and can be analyzed by comparing it to the value for the equilibrium constant (β_{eq}) for phosphate diester hydrolysis, $\beta_{eq} = -1.74$ in aqueous solution. The ratio of these values ($-1.2/-1.74 = 0.69$) provides a measure of the charge development on the leaving group in the transition state, suggesting a transition state where the leaving group oxygen carries an effective charge ($+0.74 - 1.2 = -0.46$) that is significantly more negative than in the ground state (+0.74) and comparable to that observed in solution. This is in marked contrast to the insensitivity of the D201I/D204S (k_{cat}/K_M) catalyzed reactions, where there is no change in the effective charge of the leaving group oxygen on going from the ground state in solution to the rate-limiting transition state. The WT ($k_{ST(max)}$) data show a similar insensitivity, also implying a minimal change in charge at the leaving group. However, these data cannot be analyzed in the same way as this parameter reports on the changes occurring between the enzyme−substrate and enzyme−transition state complexes, and so the starting state and equilibrium sensitivity are not known.

One way to explain the much lower Brønsted coefficients observed with the WT ($k_{ST(max)}$) and D201I/D204S FEN-catalyzed reactions is through catalytic interactions that reduce the developing charge on the leaving group in the transition state, resulting in insensitivity to changes in pK_a despite a significant degree of bond breakage in the transition state. The most common mechanism invoked for metal-dependent phosphate diesterases involves catalysis of leaving group departure by coordination of a divalent metal ion, and it is plausible that this takes place in the FEN reaction (*11*). However, metal ion catalysis should not be prevented in the K83A mutant, which does display a marked leaving group dependence. Furthermore, β_{lg} are large and negative for enzyme-catalyzed reactions where chemistry is rate limiting and metal ions are believed to be directly involved in stabilizing the scissile phosphate diester in the transition state. For example, β_{lg} of −0.8 and −0.95, respectively, have been determined for the magnesium-dependent reaction of the *Tetrahymena* ribozyme and the zinc-dependent phosphate diesterase activity of alkaline phosphatase (*31*, *34*). Thus, although such an interaction can stabilize the transition state electrostatically, it is unlikely to lead to a complete suppression of the leaving group sensitivity.

A related proposal that is frequently invoked for reactions that are insensitive to the pK_a of the leaving group is that they are general acid catalyzed. This can be achieved by using a water coordinated to a metal ion to deliver a proton to the leaving group (*35*), rather than the direct coordination of the leaving group to the ion discussed above. This is the explanation that is used to account for the characteristics of the Zn-catalyzed cleavage of alkyl 3′-uridine diesters, where the leaving group dependence is reduced to $\beta_{lg} = -0.32 \pm 0.04$ (*36*), compared to -1.28 ± 0.05 for the uncatalyzed reaction (*32*). However, even the low value for the catalyzed reaction is significantly greater than the values observed in this work, and as this type of catalysis would not be eliminated by the K83A mutation, this possibility does not explain the data. Thus, if general acid catalysis is operating in the FEN-catalyzed reaction, it is most likely to involve one of the protein residues.

In FENs a possible candidate for general acid catalysis is the positionally conserved lysine residue (K83 in T5FEN), located at the base of the helical arch protruding into the active site (*7*, *14*, *15*). This residue is present in all FENs and related DNA repair nucleases such as XPG, EXO-1, and GEN-1 enzymes (Figure S4 in Supporting Information). It has been suggested that this form of catalysis would lead to a significantly reduced Brønsted parameter; for example, the cleavage of phosphate and phosphonate monoesters catalyzed by the catalytic subunit of protein phosphatase 1, which relies on metal ion cofactors for activity, has β_{lg} of −0.32 and −0.30, respectively (*37*). These are both significantly reduced relative to the reactions in solution, although the absolute values are greater in magnitude than those observed in this report and have been rationalized in terms of general acid catalysis by a histidine residue. Suppressed β_{lg} have also been observed and interpreted similarly in enzymatic reactions that utilize phosphate diester substrates. For example, when k_{cat}/K_M was measured for the cleavage of uridine 3′-phosphate aryl esters catalyzed by bovine ribonuclease A (*38*), $\beta_{lg} = -0.17 \pm 0.03$ compared to $\beta_{lg} = -0.59$ for the reaction catalyzed by simple buffers in solution. Histidine 119 is proposed to provide the electrophilic assistance leading to this reduced charge change. However, the effect of mutating this residue to alanine showed no reduction in activity for uridine 3′-phosphate 4-nitrophenyl ester (*39*), and so it is not clear that the insensitivity of the WT-catalyzed reaction can be clearly assigned to the impact of general acid catalysis at the leaving group for these substrates. A further

complication for RNase A catalyzed reactions is that binding interactions that occur with the leaving group significantly contribute to catalytic efficiency; thus k_{cat}/K_M for uridine 3′-phosphate methyl ester is ~10^4-fold lower (*40*) than for uridine 3′-phosphate adenyl ester (r(U-p-A)), despite the similarity in leaving group pK_a. Phospholipase C catalyzes a mechanistically related transesterification proposed to involve general acid catalysis by a histidine residue. Cleavage of hydrophobic alkyl inositol monophosphates catalyzed by phospholipase C shows $\beta_{lg} = -0.12 \pm 0.11$, compared to $\beta_{lg} = -0.58 \pm 0.06$ for aryl inositol monophosphates (*41*). The lower value for the hydrophobic substrates is rationalized by invoking general acid catalysis by a histidine residue that relies on anchoring the hydrophobic moiety in a specific binding pocket. For the aryl inositol monophosphates, it is suggested that this binding interaction is weaker, leading to ineffective general acid catalysis. These data were evaluated through k_{cat} measurements and so refer to the changes that occur between the enzyme−substrate and enzyme−transition state complexes, and the possibility of rate-limiting physical steps has not been completely ruled out. Phosphate diester hydrolysis catalyzed by both of these enzymes differs from FENs in that they have no requirements for divalent metal ions and catalyze the intramolecular cyclization of their substrates.

In line with this reasoning the K83A mutant FEN, where any potential for proton donation to the leaving group by lysine 83 is abolished, does produce a notable leaving group dependence. Thus, a possible explanation for the data presented here is that the protonated form of K83 functions as a general acid, both accelerating the reaction and reducing the sensitivity to the leaving group pK_a. However, the pH-dependent behavior of the WT FEN-catalyzed EXO reaction is not readily reconciled with a role for K83 in general acid catalysis. Similarly, there is no evidence from the pH−rate profile that this form of catalysis has been abolished in the K83A mutant protein. It is possible that in the ES complex K83 titrates outside the measured data range, but a lysine residue with pK_a > 10.5 is unlikely to be a very efficient general acid.

Our preferred explanation of the data presented here is that lysine 83 acts as an electrostatic catalyst that enhances transition state binding. Reductions in rates of enzyme-catalyzed phosphoryl transfer reactions typically brought about by removal of positively charged active site residues are of 3−4 orders of magnitude (*42*−*44*), in line with the effects of K83A mutation. Although such neutralizing mutations reduce catalytic proficiency, they do not significantly reduce β_{lg}. For example, in AP the neutralizing mutation of arginine 166 to serine reduces activity toward alkyl phosphate monoester substrates by ~10^4-fold, but this change in activity does not change β_{lg} (= -0.75 ± 0.1) for catalysis by both WT and the R166S mutant (*45*).

We suggest that the EXO reaction catalyzed by WT FEN under single turnover conditions and the reaction catalyzed by the D20I/D204S mutant at low concentrations of substrate are rate limited by physical steps that mask the dependence of the chemical step on the identity of the leaving group. The physical step must be a property of the ES complex, such as a conformational change, rather than a bimolecular event such as its diffusion controlled formation. In the case of WT FEN, which does undergo a diffusion-controlled reaction at low concentrations of enzyme and substrate, the rate of a conformational change would have to be faster than the rate of dissociation of the ES complex but slower than the rate of the chemical step. This would require that phosphate diester hydrolysis proceeded with a rate $> 36 \pm 6\ s^{-1}$ for WT T5FEN, the measured maximal single turnover rate constant with the fastest HPU substrate under pH-independent conditions. Lysine 83 could significantly stabilize the transition state of the chemical step so that it is not rate limiting and its dependence on the leaving group pK_a is kinetically hidden; when that feature is removed from the active site, chemistry becomes rate limiting, and the sensitivity is revealed. By making the chemical step rate limiting, this mutation reveals something of the character of the transition state. The β_{lg} is substantially negative, implying significant bond cleavage to the leaving group in the transition state, but not greatly different from the reactions observed in solution.

In conclusion, EXO reactions catalyzed by WT FENs are rate limited by physical steps under most conditions. At low concentrations of substrate reactions are rate limited by diffusional encounter of enzyme and substrate. Although ancillary proteins (such as PCNA in higher organisms) assist FENs with target site location *in vivo*, a feature of FEN exonucleolytic reactions is that a substrate is unlikely to dissociate before chemical reaction and is thus committed to catalysis, a highly desirable property when DNA substrates are likely to prove lethal to the cell. Rate-limiting product release is also known to be a feature of FEN reactions, particularly those of larger biologically relevant substrates (*2*, *3*). But even altered proteins or reaction conditions designed to eliminate measuring product release steps or substrate association rates reveal an insensitivity to changes expected to alter the rate of the chemical reaction, suggesting a further rate-limiting physical event such as a conformational change. As the most flexible region of FEN structures is the helical arch or clamp, movement of this portion of the protein is a good candidate for the putative protein conformational change. Alternatively, substrate reorganization, in particular unpairing of the termini of FEN-bound substrates (*8*, *11*), could also be a candidate rate-limiting physical step. Further studies are required to address the role of helical arch and its conformation(s) and the structures adopted by substrates during FEN catalysis.

ACKNOWLEDGMENT

We thank Elaine Frary for expert technical assistance and Simon Thorpe for recording mass spectra. We also thank John Tainer and Brian Chapados (The Scripps Institute, La Jolla, CA) and L. David Finger (City of Hope) for informative discussions.

SUPPORTING INFORMATION AVAILABLE

Figure S1, MALDI-TOF mass spectral analysis of modified HPU substrate cleavage products; Figure S2, catalytic parameters for WT T5FEN-catalyzed hydrolysis of HP and HPU substrates at pH 9.3 and 6.5; Figure S3, effect of relative viscosity on a more complex reaction pathway; Figure S4, apositionally conserved lysine residue in all FENs and related enzymes. This material is available free of charge via the Internet at http://pubs.acs.org.

REFERENCES

1. Wu, X. T., Li, J., Li, X. Y., Hsieh, C. L., Burgers, P. M. J., and Lieber, M. R. (1996) Processing of branched DNA intermediates by a complex of human FEN-1 and PCNA. *Nucleic Acids Res. 24*, 2036–2043.
2. Williams, R., Sengerová, B., Osborne, S., Syson, K., Ault, S., Kilgour, A., Chapados, B. R., Tainer, J. A., Sayers, J. R., and Grasby, J. A. (2007) Comparison of the catalytic parameters and reaction specificities of a phage and an archaeal flap endonuclease. *J. Mol. Biol. 371*, 34–48.

3. Finger, L. D., Blanchard, S. M., Theimer, C. A., Sengerova, B., Singh, P., Chavez, V., Liu, F., Grasby, J. A., and Shen, B. (2009) The 3′-flap pocket of human flap endonuclease 1 is critical for substrate binding and catalysis. *J. Biol. Chem. 284*, 22184–22194.
4. Kaiser, M. W., Lyamicheva, N., Ma, W. P., Miller, C., Neri, B., Fors, L., and Lyamichev, V. I. (1999) A comparison of eubacterial and archaeal structure-specific 5′-exonucleases. *J. Biol. Chem. 274*, 21387–21394.
5. Huang, L., Rumbaugh, J. A., Murante, R. S., Lin, R. J. R., Rust, L., and Bambara, R. A. (1996) Role of calf RTH-1 nuclease in removal of 5′-ribonucleotides during Okazaki fragment processing. *Biochemistry 35*, 9266–9277.
6. Chapados, B. R., Hosfield, D. J., Han, S., Qiu, J. Z., Yelent, B., Shen, B. H., and Tainer, J. A. (2004) Structural basis for FEN-1 substrate specificity and PCNA-mediated activation in DNA replication and repair. *Cell 116*, 39–50.
7. Devos, J. M., Tomanicek, S. J., Jones, C. E., Nossal, N. G., and Mueser, T. J. (2007) Crystal structure of bacteriophage T4 5′ nuclease in complex with a branched DNA reveals how FEN-1 family nucleases bind their substrates. *J. Biol. Chem. 282*, 31713–31724.
8. Tomlinson, C. G., Atack, J., Chapados, B. R., Tainer, J. A., and Grasby, J. A. (2010) Substrate recognition and catalysis by flap endonucleases and related enzymes. *Biochem. Soc. Trans. 38*, 433–437.
9. Ceska, T. A., Sayers, J. R., Stier, G., and Suck, D. (1996) A helical arch allowing single-stranded DNA to thread through T5 5′-exonuclease. *Nature 382*, 90–93.
10. Dervan, J. J., Feng, M., Patel, D., Grasby, J. A., Artymiuk, P. J., Ceska, T. A., and Sayers, J. R. (2002) Interactions of mutant and wild-type flap endonucleases with oligonucleotide substrates suggest an alternative model for DNA binding. *Proc. Natl. Acad. Sci. U.S.A. 99*, 8542–8547.
11. Syson, K., Tomlinson, C., Chapados, B. R., Sayers, J. R., Tainer, J. A., Williams, N. H., and Grasby, J. A. (2008) Three metal ions participate in T5 flap endonuclease catalysed DNA hydrolysis. *J. Biol. Chem. 283*, 28741–28746.
12. Williams, A. (2003) Free Energy Relationships in Organic and Bio-organic Chemistry, The Royal Society of Chemistry, Cambridge, U.K.
13. Feng, M., Patel, D., Dervan, J. J., Ceska, T., Suck, D., Haq, I., and Sayers, J. R. (2004) Roles of divalent metal ions in flap endonuclease-substrate interactions. *Nat. Struct. Mol. Biol. 11*, 450–456.
14. Garforth, S., Ceska, T., Suck, D., and Sayers, J. (1999) Mutagenesis of conserved lysine residues in T5 5′-3′ exonuclease suggests separate mechanisms of endo- and exonucleolytic cleavage. *Proc. Natl. Acad. Sci. U.S.A. 96*, 38–43.
15. Pickering, T. J., Garforth, S. J., Sayers, J. R., and Grasby, J. A. (1999) Variation in the steady state kinetic parameters of wild-type and mutant T5 5′-3′ exonuclease with pH. Protonation of Lys-83 is critical for DNA binding. *J. Biol. Chem. 274*, 17711–17717.
16. Pickering, T. J., Garforth, S. J., Thorpe, S. J., Sayers, J. R., and Grasby, J. A. (1999) A single cleavage assay for T5 5′→3′ exonuclease: determination of the catalytic parameters for wild-type and mutant proteins. *Nucleic Acids Res. 27*, 730–735.
17. Sayers, J. R., and Eckstein, F. (1990) Properties of overexpressed phage T5 D15 exonuclease—similarities with *Escherichia coli* DNA polymerase I 5′-3′ exonuclease. *J. Biol. Chem. 265*, 18311–18317.
18. Simopoulos, T. T., and Jencks, W. P. (1994) Alkaline phosphatase is an almost perfect enzyme. *Biochemistry 33*, 10375–10380.
19. Tock, M. R., Frary, E., Sayers, J. R., and Grasby, J. A. (2003) Dynamic evidence for metal ion catalysis in the reaction mediated by a flap endonuclease. *EMBO J. 22*, 995–1004.
20. Patel, D. V., Tock, M. R., Frary, E., Feng, M., Pickering, T. J., Grasby, J. A., and Sayers, J. R. (2002) A conserved tyrosine residue aids ternary complex formation but not catalysis, in phage T5 flap endonuclease. *J. Mol. Biol. 320*, 1025–1035.
21. Fersht, A. R. (1985) Enzyme Structure and Mechanism, 2nd ed., W. H. Freeman, New York.
22. Cornish-Bowden, A. (1995) Fundamentals of Enzyme Kinetics, Portland Press, London.
23. Åström, H., Limén, E., and Strömberg, R. (2004) Acidity of secondary hydroxyls in ATP and adeonsine analogues and the question of a 2′-3′-hydrogen bond in ribonucleosides. *J. Am. Chem. Soc. 126*, 14710–14711.
24. Berg, O. G., and von Hippel, P. H. (1985) Diffusion-controlled macromolecular interactions. *Annu. Rev. Biophys. Biophys. Chem. 14*, 131–160.
25. Brouwer, A. C., and Kirsch, J. F. (1982) Investigation of diffusion-limited rate of chymotrypsin reactions by viscosity variation. *Biochemistry 21*, 1302–1307.
26. Hodskinson, M. R., Allen, L. M., Thomson, D. P., and Sayers, J. R. (2007) Molecular interactions of *Escherichia coli* ExoIX and identification of its associated 3′-5′ exonuclease activity. *Nucleic Acids Res. 35*, 4094–4102.
27. Xu, Y., Derbyshire, V., Ng, K., Sun, X., Grindley, N., and Joyce, C. (1997) Biochemical and mutational studies of the 5′-3′ exonuclease of DNA polymerase I of *Escherichia coli*. *J. Mol. Biol. 268*, 284–302.
28. Bastock, J., Webb, M., and Grasby, J. A. (2007) The pH-dependence of the *Escherichia coli* RNase HII-catalysed reaction suggests that an active site carboxylate participates directly in catalysis. *J. Mol. Biol. 368*, 421–433.
29. Baldwin, G. S., Erskine, S. G., and Halford, S. E. (1999) DNA cleavage by the *Eco*RV restriction endonuclease: roles of divalent metal ions in specificity and catalysis. *J. Mol. Biol. 288*, 87–103.
30. Campbell, F. E., Cassano, A. G., Anderson, V. E., and Harris, M. E. (2002) Pre-steady-state and stopped-flow fluorescence analysis of *Escherichia coli* ribonuclease III: insights into mechanism and conformational changes associated with binding and catalysis. *J. Mol. Biol. 317*, 21–40.
31. Zalatan, J. G., and Herschlag, D. (2006) Alkaline phosphatase mono- and diesterase reactions: comparative transition state analysis. *J. Am. Chem. Soc. 128*, 1293–1303.
32. Kosonen, M., Yousefi-Saladekh, Y., Strömberg, R., and Lönnberg, H. (1997) Mutual isomerization of uridine 2′- and 3′-alkylphosphates and cleavage to a 2′,3′-cyclic phosphate: the effect of the alkyl group on the hydronium- and hydroxide-ion-catalyzed reactions. *J. Chem. Soc., Perkin Trans. 2,* 2661–2666.
33. Kirby, A. J., and Younas, M. (1970) The reactivity of phosphate esters. Diester hydrolysis. *J. Chem. Soc. B,* 510–513.
34. Herschlag, D., Eckstein, F., and Cech, T. R. (1993) The importance of being ribose at the cleavage site in the *Tetrahymena* ribozyme reaction. *Biochemistry 32*, 8312–8321.
35. Horton, N. C., Connolly, B. A., and Perona, J. J. (2000) Inhibition of EcoRV endonuclease by deoxyribo-3′-S-phosphorothiolates: a high-resolution X-ray crystallographic study. *J. Am. Chem. Soc. 122*, 3314–3324.
36. Mikkola, S., Stenman, E., Nurmi, K., Yousefi-Salakdeh, E., Strömberg, R., and Lönnberg, H. (1999) The mechanism of the metal ion promoted cleavage of RNA phosphodiester bonds involves a general acid catalysis by the metal aquo ion on departure of the leaving group. *J. Chem. Soc., Perkin Trans. 2,* 1619–1625.
37. McWhirter, C., Lund, E. A., Tanifum, E. A., Feng, G., Sheikh, Q. I., Hengge, A. C., and Williams, N. H. (2008) Mechanistic study of protein phosphatase-1 (PP1), a catalytically promiscuous enzyme. *J. Am. Chem. Soc. 130*, 13673–13682.
38. Davis, A. M., Regan, A. C., and Williams, A. (1988) Experimental charge measurement at leaving oxygen in the bovine ribonuclease A catalysed cyclisation of uridine 3′-phosphate aryl esters. *Biochemistry 27*, 9042–9047.
39. Thompson, J. E., and Raines, R. T. (1994) Value of general acid-base catalysis to ribonuclease A. *J. Am. Chem. Soc. 116*, 5467–5468.
40. Witzel, H., and Barnard, E. A. (1962) Mechanism and binding sites in the ribonuclease reaction. II. Kinetic studies of the first step of the reaction. *Biochem. Biophys. Res. Commun. 7*, 295–299.
41. Mihai, C., Kravchuk, A. V., Tsai, M.-D., and Bruzik, K. S. (2003) Application of Bronsted-type LFER in the study of the phospholipase C mechanism. *J. Am. Chem. Soc. 125*, 3236–3242.
42. Mossakowska, D., Kerstin, N., and Fersht, A. (1989) Kinetic characterization of the recombinant ribonuclease from *Bacillus amyloliquefaciens* (Barnase) and investigation of key residues in catalysis by site-directed mutagenesis. *Biochemistry 28*, 3843–3850.
43. Serpersu, E. H., Shortle, D., and A.S., M. (1987) Kinetic and magnetic resonance studies of active-site mutants of staphylococcal nuclease: factors contributing to catalysis. *Biochemistry 26*, 1289–1300.
44. Thompson, J. E., Kutateladze, T. G., Schuster, M. C., Venegas, F. D., Messmore, J. M., and Raines, R. T. (1995) Limits to catalysis by ribonuclease A. *Bioorg. Chem. 23*, 471–481.
45. O'Brien, P. J., and Herschlag, D. (1999) Does the active site arginine change the nature of the transition state for alkaline phosphatase-catalysed phosphoryl transfer? *J. Am. Chem. Soc. 121*, 11022–11023.